Bioorganic & Medicinal Chemistry 20 (2012) 933–941

Contents lists available at SciVerse ScienceDirect

Bioorganic & Medicinal Chemistry

journal homepage: www.elsevier.com/locate/bmc

Cell-based and in-silico studies on the high intrinsic activity of two boron-containing salbutamol derivatives at the human β_2-adrenoceptor

Marvin A. Soriano-Ursúa [a,*], Daniel A. McNaught-Flores [b], Gustavo Nieto-Alamilla [b], Aldo Segura-Cabrera [c], José Correa-Basurto [a], José A. Arias-Montaño [b], José G. Trujillo-Ferrara [a]

[a] Departamentos de Fisiología, Bioquímica Médica y Sección de Estudios de Posgrado e Investigación, Escuela Superior de Medicina, Instituto Politécnico Nacional, Plan de San Luis y Díaz Mirón, Col. Casco de Santo Tomás, Del. Miguel Hidalgo, 11340 México, D.F., Mexico
[b] Departamento de Fisiología, Biofísica y Neurociencias, Centro de Investigación y de Estudios Avanzados del IPN, Av. IPN 2508, 07360 México, D.F., Mexico
[c] Centro de Biotecnología Genómica, Boulevard del Maestro Esq. Elías Piña, Col. Narciso Mendoza, C.P. 88710 Cd. Reynosa, Tamaulipas, Mexico

ARTICLE INFO

Article history:
Received 23 August 2011
Revised 16 November 2011
Accepted 23 November 2011
Available online 1 December 2011

Keywords:
Beta adrenergic receptor agonists
7TM
Boron
Drug–receptor interaction
Allosteric modulation

ABSTRACT

Salbutamol is a well-known β_2 adrenoceptor (β_2AR) partial agonist. We synthesized two boron-containing salbutamol derivatives (BCSDs) with greater potency and efficacy, compared to salbutamol, for inducing β_2AR-mediated smooth-muscle relaxation in guinea-pig tracheal rings. However, the mechanism involved in this pharmacological effect remains unclear. In order to gain insight, we carried out binding and functional assays for BCSDs in HEK-293T cells transfected with the human β_2AR (hβ_2AR). The transfected hβ_2AR showed similar affinity for BCSDs and salbutamol, but adenosine 3′,5′-cyclic phosphate (cAMP) accumulation induced by both BCSDs was similar to that elicited by isoproterenol and greater than that induced by salbutamol. The boron-containing precursors (boric and phenylboronic acids, 100 μM) had no significant effect on salbutamol binding or salbutamol-induced cAMP accumulation. These experimental results are in agreement with theoretical docking simulations on lipid bilayer membrane-embedded hβ_2AR structures. These receptors showed slightly higher affinity for BCSDs than for salbutamol. An essential change between putative active and inactive conformational states depended on the interaction of the tested ligands with the fifth, sixth and seventh transmembrane domains. Overall, these data suggest that BCSDs induce and stabilize conformational states of the hβ_2AR that are highly capable of stimulating cAMP production.

1. Introduction

The design and synthesis of drugs acting as agonists at β_2-adrenoceptors (β_2ARs) is a topic of high pharmacological interest due to their clinical use as smooth-muscle relaxants.[1,2] Salbutamol (also named albuterol) is a well-known βAR partial agonist with selectivity for the β_2- over the β_1- and β_3-subtypes (21- and 5-fold selectivity, respectively).[3] We previously reported the synthesis of two boron-containing salbutamol derivatives (BCSDs) which possess greater potency and efficacy than its precursor for inducing β_2AR-mediated smooth-muscle relaxation in guinea-pig tracheal rings.[4,5]

This effect can be partially explained by the higher affinity predicted on tridimensional models of human and guinea-pig β_2ARs, along with a good capability for interacting with key residues located in the fifth transmembrane domain of the receptor.[4–7] The boron atom has chemical properties that could play an essential role in BCSD–β_2AR interactions, as proposed for other proteins with similar amino acid disposition in their interaction site.[7–9] However, additional studies are required for elucidating the mechanism involved in the greater BCSD-induced, β_2AR-mediated relaxant effect. In this regard, our understanding about the interactions between BCSDs and the β_2AR could be improved by employing recent structural data on the interaction of ligands exhibiting different intrinsic efficacy with seven-transmembrane domain receptors (7TM; also named G protein coupled receptors or GPCRs)[10–13] in computational procedures applied to the recently elucidated β_2AR-G protein complex.[14] In previous studies, we have found a close relationship between experimental and theoretical results in relation to the mechanisms of the β_2AR.[4,5]

With the aim of predicting key interactions which could help to explain the pharmacological behavior of BCSD-β_2AR complexes, we carried out binding and functional assays of the new BCSDs and their precursors in HEK-293T cells transfected with the human β_2AR (hβ_2AR), and docking studies on the lipid bi-layer embedded hβ_2AR (in putative inactive or active states) in interaction with the boron-containing compounds and their precursors.

* Corresponding author. Fax: +52 555 7296000/62747.
E-mail address: msoriano@ipn.mx (M.A. Soriano-Ursúa).

0968-0896/$ - see front matter © 2011 Elsevier Ltd. All rights reserved.
doi:10.1016/j.bmc.2011.11.054

2. Material and methods

2.1. Materials

The following compounds were purchased from Sigma (St. Louis, MO): adenosine 3′,5′-cyclic phosphate (cAMP), (±)-isoproterenol hydrochloride, *R*-(−)salbutamol, boric acid (BA), phenylboronic acid (PBA), protein kinase A (PKA, regulatory subunit), and ICI-118,551 ((±)-1-[2,3-(dihydro-7-methyl-1H-inden-4-yl)oxy]3-[(1-methylethyl)amino]2-butanol hydrochloride). BR-AEA (1-(4-di-hydroxy-3,5-dioxa-4-borabicyclo[4.4.0]deca-7,9,11-trien-9-yl)-2-(*tert*-butylamino)ethanol) and boronterol ((*R*)-4-(2-(*tert*-butylamino)-1-hydroxyethyl)-2-(hydroxymethyl)phenyl hydrogen phenylboronate) were synthesized in our laboratory as described elsewhere.[4,5] [Methyl-^{3}H]-dihydroalprenolol ([^{3}H]-DHA, specific activity 111.8 Ci/mmol) and [2,8-^{3}H]-adenosine 3′,5′-cyclic phosphate ([^{3}H]-cAMP, 34 Ci/mmol) were from Perkin Elmer (Boston, MA). The plasmid pcDNA3.1-hβ_2AR was from Missouri S&T cDNA Resource Center (www.cdna.org).

2.2. Cell culture and transfection

HEK-293T cells were grown in Dulbecco's modified Eagle's medium (DMEM) supplemented with 10% bovine fetal serum, penicillin (50 UI/mL) and streptomycin (0.1 mg/mL) under a humidified atmosphere (5% CO_2) at 37 °C.

Cells were transiently transfected with the plasmid pcDNA3.1-hβ_2AR and linear 25 KDa polyethylenimine (PEI). Briefly, the plasmid (0.25 μg/10^6 cells) was mixed with PEI (5 μL of a sterile 1 mg/mL solution per 10^6 cells) in 300 μL serum-free DMEM and incubated for 30 min at room temperature. The mixture was added to 5 mL of a cell suspension (10^6 cells/mL) and the tube was then placed into a CO_2 incubator. After 30 min 5 mL of growth medium were added and the cell suspension was seeded in Petri dishes (10 cm diameter) or 24 well-plates as required. All assays were performed 24 h after transfection.

2.3. [^{3}H]-DHA) binding to cell membranes

Transfected HEK-293T cells, grown in Petri dishes, were lyzed by incubation (20 min, 4 °C) in hypo-osmotic buffer (10 mM Tris-HCl, 1 mM EGTA, pH 7.4). After centrifugation (42,000*g*, 20 min) the resulting pellet was re-suspended (~1 mg protein/mL) in incubation buffer (50 mM Tris–HCl, pH 8). [^{3}H]-DHA binding assays were carried out as described in detail elsewhere.[15]

2.4. Measurement of cAMP accumulation in intact cells

Transfected HEK-293T cells, grown in 24-well plates, were washed twice with phosphate-buffered saline solution (PBS) before incubation (37 °C) in 240 μL PBS containing 1 mM IBMX (3-isobutyl-1-methylxantine). After 15 min, drugs were added in a 10-μL volume and incubations continued for another 30 min. The composition of the PBS solution was (mM): NaCl 137, KCl 2.7, Na_2HPO_4 10, KH_2PO_4 1.76, $MgCl_2$ 1, and $CaCl_2$ 1 at pH 7.4. Incubations were terminated with 25 μL ice-cold 1 N HCl and samples were neutralized with 25 μL ice-cold 1 N NaOH and 100 μL 1 M Tris–HCl (pH 7.4). Endogenous cAMP was determined in 50-μL samples by determining the inhibition of [^{3}H]-cAMP binding to the regulatory subunit of PKA, essentially as described in detail elsewhere.[16] Briefly, samples were incubated in 125 μL of incubation buffer containing protein kinase A (PKA) and [^{3}H] cAMP (10 nM). After 2.5 h at 4 °C, incubations were terminated by filtration over GF/C filters and by three subsequent washes with 1 mL ice-cold deionized water. Retained radioactivity was determined by liquid scintillation and the amount of cAMP in each sample was calculated using a standard cAMP curve (10^{-12}–10^{-6} M). The composition of the incubation buffer was (mM): Tris–HCl 50, NaCl 100, EDTA 5 (pH 7.2 at 4 °C).

2.5. Molecular modeling

Two hβ_2AR 3D structures retrieved from protein data bank (PDB) were used in this study: the one described by Cherezov et al. (PDB ID: 2RH1)[10] obtained in complex with an inverse agonist, and the structure reported by Rossenbaum et al. (PDB ID: 3PDS), obtained in complex with an irreversible agonist.[12] Ligands, the T4-lysozyme and co-crystallized water molecules were removed from the hβ_2AR structures and the protein hydrogen atoms were added before submitting these receptors to molecular dynamics (MDs) simulations (to explore their different conformation movements) and docking analysis.

2.6. Molecular dynamics protocol

With the aim of gaining insight into specific interactions of BCSDs and their precursors in hβ_2AR binding and activation processes, we considered the analysis on inactive and active hβ_2AR structures (PDB codes: 2RH1 and 3PDS, respectively). Additionally, initial changes in the hβ_2AR were studied by comparing its structure immediately after embedding this receptor on a bilayer lipid membrane with the structure found after 30 ns of MD simulations, as such initial changes could be elemental in the activation processes observed in previous simulations.[12,17]

For this purpose, all simulations were performed using the gromacs software package, version 4.5.3.[18] A pre-equilibrated 1-palmitoyl-2-oleoyl-phosphatidylcholine (POPC) bilayer with 128 lipid molecules was downloaded from Tieleman's group electronic page: (http://moose.bio.ucalgary.ca/index.php?page=Structures_and_Topologies). The protein was embedded in the pre-equilibrated POPC lipid bilayer using inflategro perl script from Tieleman's group and several rounds of energy minimization were performed. After 23 iterations of scaling down by 0.95, an area per lipid of ~74 Å^2 was yielded, a figure above the experimental value of ~66 Å^2. The main reason for this difference is that inflategro script tends to overestimate the area per lipid,[19] but the value obtained was good enough to proceed to the equilibration procedure.

All systems were equilibrated using simulated-annealing under an isothermal–isobaric (NPT) ensemble for 500 ps. The LINCS method[20] was used to restrain all protein heavy atoms in any direction, and on the phosphorus atoms of the lipid head groups in the vertical (*z*) direction allowing a 2 fs integration step. The use of simulated-annealing under NPT ensemble prevented the formation of solvent voids that distort the dimensions of the unit cell.

Following simulated-annealing, isothermal-isobaric (NPT) equilibration was performed for 500 ps, applying a pressure of 10 MPa in the transverse direction and 0.1 MPa in the vertical direction. Water, lipids and protein were coupled separately to a temperature bath at 300°K with a relaxation time (τT) of 0.2 ps using a Berendsen thermostat.[21] Each group (protein/cholesterol, lipids, and solvent/ions) was coupled to a separate temperature bath.

The parameters developed by Berger et al.[22] were applied to the POPC lipids, and the gromos96 53a6 parameter set was used to describe the rest of the system (protein, solvent, ions). Lennard–Jones interactions were cut-off at 1.4 nm, and short-range, non-bonded interactions were calculated with a twin-range cut-off scheme (0.9/1.4 nm), with the neighbor list updated every five simulation steps. Electrostatic interactions were calculated using the particle mesh Ewald algorithm[23] with fourth-order spline interpolation

and a Fourier grid spacing of 0.12 nm. This treatment of electrostatics has been shown to provide an accurate representation of lipid properties,[24] and is also commonly used in simulations of proteins. Following the 1000 ps of equilibration, production MD was conducted for 30 ns, using an NPT ensemble. A pressure of 0.1 MPa was applied in all directions, with all other parameters being the same as in the NPT equilibration. All position restraints were removed prior to the production phase. Simulations were conducted using the Argentum cluster of Centro Nacional de Supercómputo. Coordinates were saved every 2 ps for analysis, which was performed using tools included in the gromacs package. The molecular topology for cholesterol was generated by GlycoBioChem PRODRG2 server[25] at http://davapc1.bioch.dundee.ac.uk/prodrg/.

2.7. Ligand retrieval

All compounds depicted in Figure 1 were docked on the hβ_2AR. For each ligand the 3D structure was built and geometrically optimized at the B3LYP/6-31G* level with Gaussian 03 software.[26]

2.8. Docking methodology

To identify the hβ_2AR recognition sites and determine ligand affinities, docking simulations were performed using 3D ligand/receptor structures. To corroborate the availability of the putative binding site in the refined model, a binding site prediction was previously carried out with the Q-site Finder program.[27]

All rigid/flexible bonds, partial atomic charges (Gasteiger–Marsili formalism), and non-merge hydrogens of the ligands were assigned. The Kollman partial charges for all atoms in the hβ_2AR, and the non-merge hydrogens were added using AutoDock Tools 1.5.0, maintaining the rest of the other program's default parameters.[28,29] Docking simulations were performed using a commonly-used search algorithm (hybrid Lamarckian Genetic) implemented on AutoDock 4.0.1.[29] The initial population was of 100 randomly-placed individuals, and the maximum number of energy evaluations was 10 million. To search for all potential binding sites on the hβ_2AR, input initializations of the ligand structures and hβ_2AR binding site definitions were carried out using a GRID-based procedure.[30] A blind docking procedure using a box of $70 \times 70 \times 70$ Å point grid with 0.375-Å spacing was used, centered in the midpoint between α-carbon of the conserved amino acids Asp113 and Ser204. Docked orientations within a root-mean square deviation of 0.5 Å were clustered together and the lowest free-energy cluster returned for each compound was used for further analysis using AutoDock Tools 1.5.0. Docking results (hβ2AR-ligand complexes) were visualized using VMD 1.8.7.[31] The free energy and K_i values yielded from Autodock program were considered for estimating affinity values as elsewhere.[4–6]

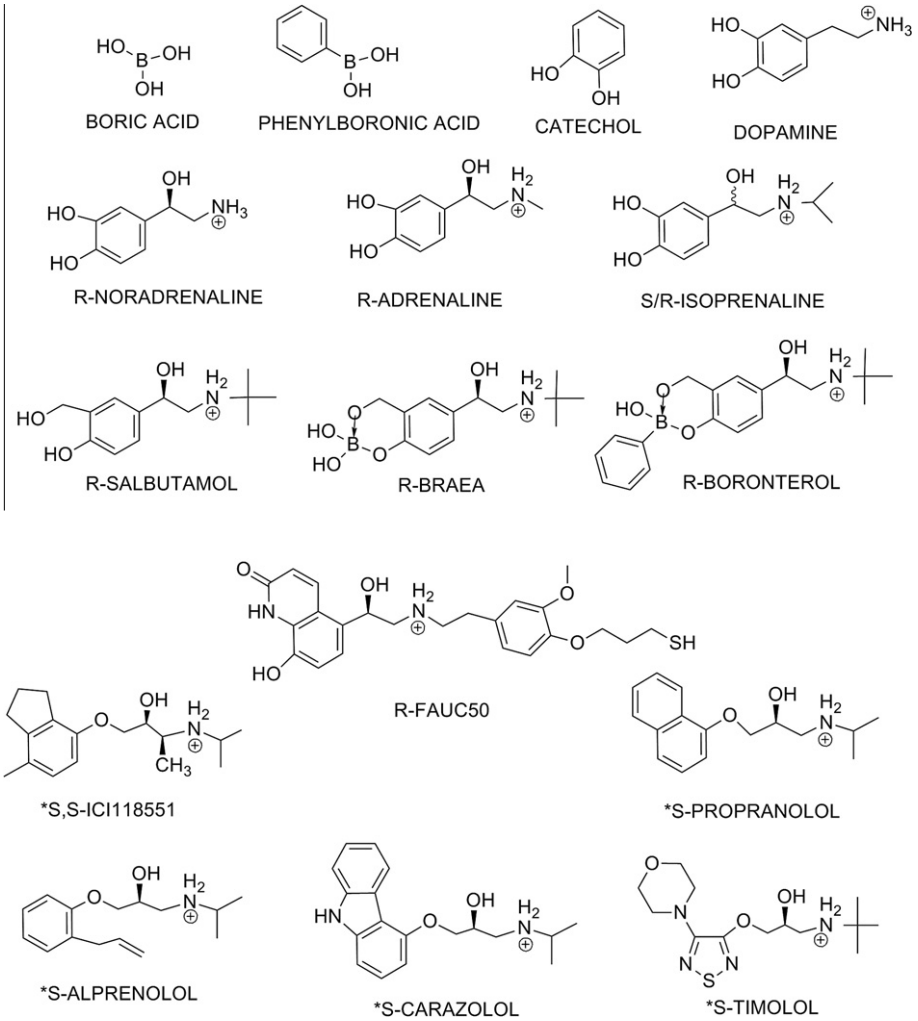

Figure 1. Compounds tested as hβ_2AR ligands in this study. Asterisk indicates antagonists or inverse agonists.

3. Results

3.1. Functional studies

3.1.1. Expression of hβ$_2$-AR by transfected HEK-293T cells

Transfected HEK-293T cells (HEK-293T-hβ$_2$AR) expressed high levels of the hβ$_2$-AR, as assessed by saturating [^{3}H]-DHA binding with maximum binding (B_{max}) 7.60 ± 1.59 pmol/mg protein (mean ± s.e.m. from four determinations) and by calculating dissociation constant (K_d) 1.09 ± 0.16 nM (Supplementary Fig. 1).

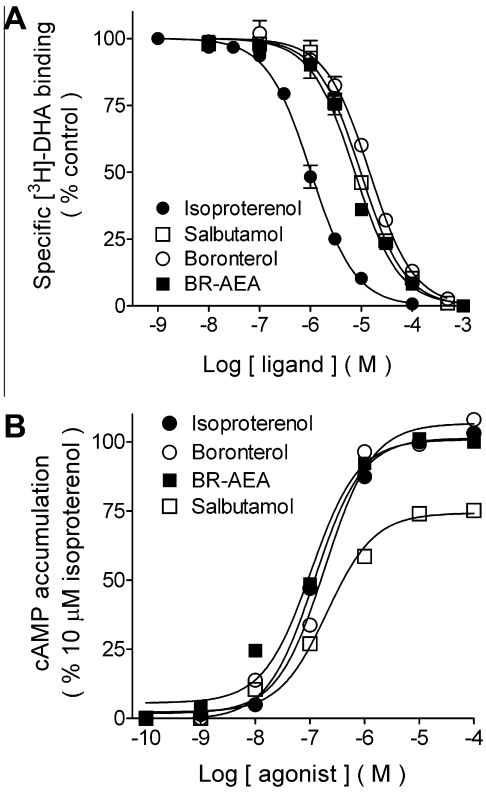

Figure 2. Agonist effects on [^{3}H]-DHA binding and cAMP accumulation in HEK-293T cells transiently transfected with the hβ$_2$AR. (A) Inhibition of [^{3}H]-DHA binding. Membranes from transfected HEK-293T cells were incubated with 1 nM [^{3}H]-DHA and the indicated concentrations of agonists. Values are expressed as percentage of specific binding of the control and are the mean ± s.e.m. of triplicate determinations from a representative experiment, repeated three times with similar results. The line drawn is the best fit to a logistic equation for a one-site binding model. K_i and pK_i values calculated from the best-fit IC_{50} estimates are given in the text. (B) Agonist-induced cAMP accumulation. Transfected HEK-293T cells were pre-incubated (15 min) with 1 mM IBMX and then exposed for 30 min to the indicated concentrations of agonists. Values are averages of duplicates from a representative experiment, repeated three times with similar results. The line drawn is the best fit to a logistic equation. EC_{50} and pEC_{50} values are given in Table 1.

3.1.2. Effect of salbutamol and BCSDs on [^{3}H]-DHA binding and cAMP accumulation

The full βAR agonist isoproterenol, the partial agonist salbutamol and two BCSDs (BR-AEA and boronterol) all inhibited the binding of [^{3}H]-DHA to membranes from HEK-293T-hβ$_2$AR cells in a concentration-dependent manner (Fig. 2). While isoproterenol was significantly more potent than the other three drugs (7.76- to 13.18-fold, P <0.05, ANOVA and Tukey's test, Table 1), no significant differences were found among salbutamol, BR-AEA and boronterol.

In functional assays salbutamol, BR-AEA and boronterol showed similar potency to stimulate cAMP accumulation, and their potencies were slightly higher (but not statistically different) than that observed for isoproterenol (Table 1). While the maximum effect of salbutamol was significantly lower than that of isoproterenol (75 ± 7%, P <0.05, ANOVA and Dunnett's test), there was no significant difference between either BR-AEA or boronterol and isoproterenol in this sense. These two boron-containing compounds yielded 99 ± 7% and 99 ± 6% of the isoproterenol effect, respectively (Fig. 2, Table 1). The analysis of agonist efficacy by two different approaches (Table 1) showed that boronterol, but not BR-AEA, had a larger intrinsic efficacy when compared with salbutamol.

3.1.3. Effect of boric and phenyl-boronic acids on salbutamol-induced cAMP accumulation

BCSDs may release their precursor acids upon dissolution in aqueous solutions, thus affecting BCSD binding to the hβ$_2$AR and the functional output. Consequently, we tested the effect of both acids on salbutamol inhibition of [^{3}H]-DHA binding and agonist-induced cAMP accumulation. Neither acid significantly modified the potency of salbutamol to inhibit [^{3}H]-DHA binding when tested at 100 μM (Fig. 3). At the same concentration both acids moderately reduced salbutamol-induced cAMP accumulation (to 76 ± 16% and 75 ± 11% of the accumulation with salbutamol alone for boric and phenylboronic acids, respectively), but the effect did not yield statistical significance (P >0.05, ANOVA and Dunnett's test). In both cases the error is large, reflecting the variability from one determination to another. The salbutamol potency was also decreased by both acids (a 1.9-fold reduction by boric acid and 3.1-fold by phenylboronic acid) and although the differences did not yield statistical significance (P >0.05, ANOVA and Dunnett's test). The reduction in maximum effect and potency values was reflected in decreased agonist efficacy (Table 2).

3.2. Molecular modeling

3.2.1. Inactive and active β$_2$AR conformations and the effects of membrane embedding

Compared to original hβ$_2$AR structures, we observed subtle conformational changes in membrane embedded structures and after the 30 ns of MD simulations. The RMSD changes (not greater than 3.94 Å) were essentially due to the rotation of TM6 and TM7 towards TM3, and were greater in the MD simulation for the hβ$_2$AR

Table 1
Constants for agonist inhibition of [^{3}H]-DHA binding and stimulation of cAMP accumulation in HEK-293T cells transiently transfected with the hβ$_2$-AR

	Inhibition of [^{3}H]-DHA binding		cAMP accumulation		R_{max} (% iso)	Agonist efficacy	
	K_i (nM)	pK_i	EC_{50} (nM)	pEC_{50}		Coupling efficiency[a]	Relative efficacy[b]
Isoproterenol	501	6.30 ± 0.09 (3)	240	6.62 ± 0.07 (4)	100	0.143	2.088
Boronterol	6,607	5.18 ± 0.06 (3)	138	6.86 ± 0.14 (4)	99 ± 6	6.168	47.40
BR-AEA	3,890	5.41 ± 0.03 (3)	166	6.78 ± 0.05 (3)	99 ± 7	2.952	23.20
Salbutamol	5,623	5.25 ± 0.07 (3)	145	6.84 ± 0.17 (4)	75 ± 7	4.971	29.08

Values are means or means ± s.e.m. from the number of experiments indicated between parenthesis.
[a] Coupling efficiency (CE) was determined using the formula CE = (Ki − EC_{50})/(EC_{50})r,[53] where r corresponds to receptor number.
[b] Relative efficacy (RE) was estimated as RE = E_{max} (K_i/EC_{50}).[54]

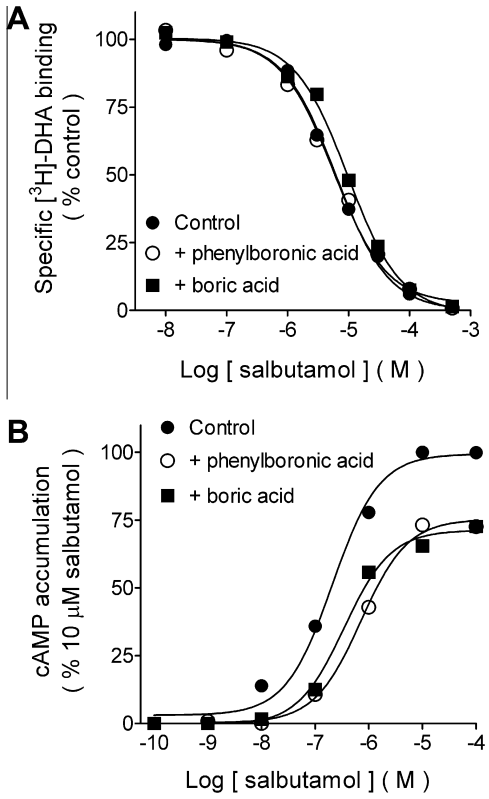

Figure 3. Effect of phenylboronic acid and boric acid on salbutamol inhibition of [^{3}H]-DHA binding and stimulation of cAMP accumulation in HEK-293T cells transiently transfected with the hβ_2AR. (A) Inhibition of [^{3}H]-DHA binding. Membranes from transfected cells were incubated with 1 nM [^{3}H]-DHA and the indicated concentrations of salbutamol in the presence and absence of phenylboronic acid or boric acid (100 μM). Values are expressed as percentage of specific binding of the control and are averages of duplicates from a representative experiment, repeated two times with similar results. The line drawn is the best fit to a logistic equation for a one-site binding model. K_i and pK_i values calculated from the best-fit IC_{50} estimates are given in the text. (B) Salbutamol-induced cAMP accumulation. Transfected cells were pre-incubated (15 min) with 1 mM IBMX and then exposed for 30 min to the indicated concentrations of salbutamol in the presence and absence of phenylboronic acid or boric acid (100 μM). Values are averages of duplicates from a representative experiment, repeated three times with similar results. The line drawn is the best fit to a logistic equation. EC_{50} and pEC_{50} values are given in the text.

active form (Supplementary Figs. 2 and 3), in agreement with changes in distance between TM3 and TM6 or TM7 for the 3PDS structure. However, neither the distance between TM3 and TM7 nor that between residues constituting the 'ionic lock' (Arg131 and Glu268) were significantly affected (change $\leqslant$2.85 Å) after membrane embedding or MD simulations (Supplementary Fig. 4). The rotation of specific residues is discussed in the corresponding section.

3.2.2. Ligand interactions with inactive or active hβ_2ARs

Docking simulations yielded adequate binding conformations and showed high reproducibility of the crystallized ligand on the hβ_2AR binding site. Ligands with known intrinsic activity (i.e. agonists or antagonists) were capable of reaching the so-called 'main' or orthosteric binding site, which involves residues from TM3 to TM7. This in agreement with what has been observed on hβ_2AR structures with several reported approaches.[32–34] Consequently, these ligands showed interactions with residues TM3 to TM7 and with some residues of second extracellular loop. However, in the highest affinity complexes, boric and phenylboronic acids were only able to reach a region that is shallower than the orthosteric site.

3.2.3. Affinity estimation and selectivity of ligands

The estimated affinity correlated with our previous experimental estimation and with similar docking procedures.[4,5] The coefficient of determinations in linear regression for theoretical–experimental values was in the range 0.675–0.893 for all ligands tested on the four structures employed in this study, but no greater correlation was observed for agonists or antagonists (or inverse agonists) on any particular hβ_2AR structure, nor did agonists have higher affinity on putative active models or antagonists on inactive models. All affinity values were underestimated by 2–3 orders of magnitude, that is, the predicted pK_d values were 100- to 1000-fold lower than the experimental estimates.

In contrast, there were differences in the residues that interacted with agonists or antagonists on active or inactive models in comparison with previous reports.[4,7,33] For example, agonists formed hydrogen bonds with residues Ser203, Ser204 and/or Ser207 in TM5, and there were a greater number of interactions with residues in TM6 and TM7, whereas antagonists and inverse agonists interacted with the same residues in TM3 and TM5, but with different residues in TM6 and TM7.

Focusing on the BCSDs, their boron-containing precursors and the experimentally employed hβ_2AR ligands, we analyzed the predicted affinity on hβ_2AR models. Considering the highest affinity values in the ligand-hβ_2AR complexes, we found that the calculated affinity of salbutamol was lower than that for isoproterenol, which was in agreement with in vitro assays. However, the model described by Cherezov[10] after membrane-embedding led to different calculated affinities. The BCSD precursors (boric and phenylboronic acids) showed at least 100-fold lower affinity than BCSDs, salbutamol or isoproterenol (Table 2). BR-AEA showed similar or lower affinity than salbutamol, and boronterol showed affinity in a range similar to that for salbutamol (Fig. 4).

3.3. Particular BCSD interactions on hβ_2AR adrenoceptor

Boronterol and BR-AEA docked in the main binding site for catecholamines, reaching the hydrophobic cavity formed by residues of TM3 to TM7. Their amine moiety showed electrostatic interaction

Table 2
Constants for salbutamol inhibition of [^{3}H]-DHA binding and stimulation of cAMP accumulation in the presence of boric and phenylboronic acids

	Inhibition of [^{3}H]-DHA binding		cAMP accumulation		R_{max} (% salbutamol)	Agonist efficacy	
	K_i (nM)	pK_i	EC_{50} (nM)	pEC_{50}		Coupling efficiency[a]	Relative efficacy[b]
Salbutamol	5,623	5.25 ± 0.07 (3)	145	6.84 ± 0.17 (4)	100	4.971	38.779
Salbutamol + boric acid	3,802	5.42 ± 0.15 (3)	275	6.56 ± 0.22 (4)	76 ± 16	1.688	10.507
Salbutamol + phenylboronic acid	4,677	5.33 ± 0.07 (3)	457	6.34 ± 0.11 (3)	75 ± 11	1.215	7.676

When required boric and phenylboronic acids were present at 100 μM. Values are means or means ± s.e.m. from the number of experiments indicated between parenthesis.
[a] Coupling efficiency (CE) was determined using the formula $CE = (K_i - EC_{50})/(EC_{50})r$,[53] where r corresponds to receptor number.[53]
[b] Relative efficacy (RE) was estimated as $RE = E_{max}(K_i/EC_{50})$.[54]

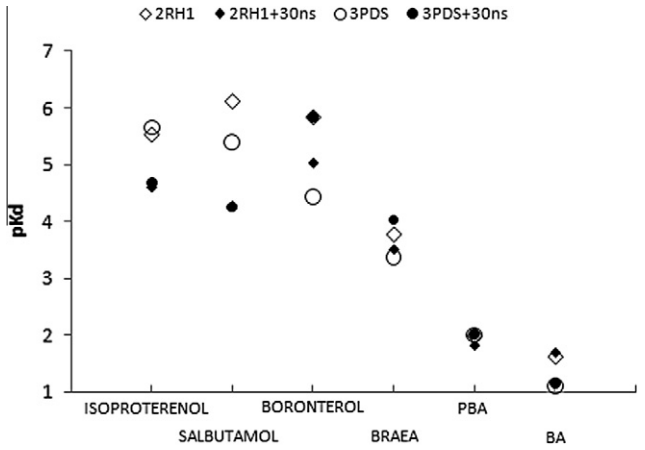

Figure 4. Estimated affinity of compounds employed experimentally in this study. Boronterol and BRAEA are boron containing salbutamol derivatives (BCSD), while phenylboronic (PBA) and boric (BA) acids are their respective boron containing precursors.

with Asp113 and their *tert*-butyl moiety was oriented to the upper segment of TM7. In addition, both BCSDs showed a large number of interactions by hydrogen bonds with Ser203, Ser204 and/or Ser207 residues in TM5 in both hβ_2AR structures (Fig. 5).

On the other hand, both boric and phenylboronic acids interacted with the receptor surface exposed just below the second extracellular loop (Fig. 6). However, in the highest affinity complexes (with greatest score in the docking simulations), boric acid interacts with the region above the TM7 with residues Cys191, Asp192 and Lys305, while phenylboronic acid interacted with a region located above the TM3, in a crevice formed among residues Asn103, Cys106, Glu107, Tyr174 and Arg175. These two sites—for boric and phenylboronic acids—share a common pattern, that of the existence of a basic and an acid residue near each other (Fig. 6).

4. Discussion

4.1. Experimental approach

Our results indicate that in membranes of transfected HEK-293T cells expressing high levels of hβ_2ARs, the potency of BCSDs to inhibit [^{3}H]-DHA binding is similar to that of salbutamol but lower than that of isoproterenol. The high receptor expression augmented the probability of either inactive or G protein-uncoupled conformations of the hβ_2AR, leading to K_i and EC_{50} values larger than those reported elsewhere.[3,10,15] In line with this, the pEC_{50} value for isoproterenol-induced cAMP accumulation in HEK-293T-hβ_2AR cells (6.62 ± 0.07) was similar to the estimate (6.89 ± 0.10) obtained in human prostate cancer DU-145 cells that endogenously express a much lower density of β_2ARs (22.7 fmol/mg protein).[15] Further, the shift in the agonist-response curve from the agonist-binding curve is much larger for salbutamol and both BCSD than for isoproterenol (Table 1), suggesting that agonists bind to and stabilize different conformational states of the β_2AR. In light

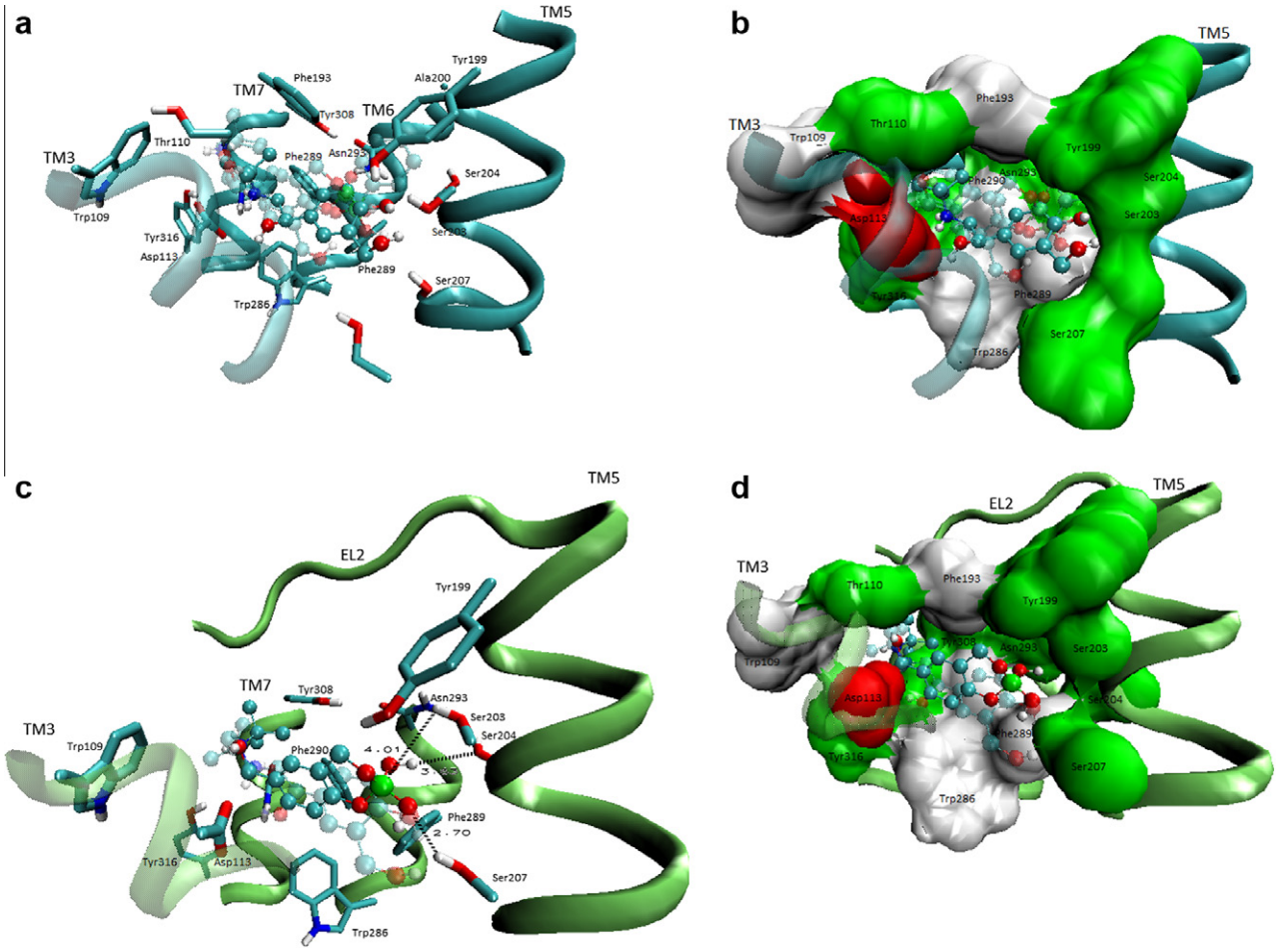

Figure 5. View of salbutamol and BCSDs (partial/full agonists) on inactive (a and b) or active (c and d) hβ_2AR. In panel C some viable hydrogen bonds and boron interactions are labeled with distance in Å.

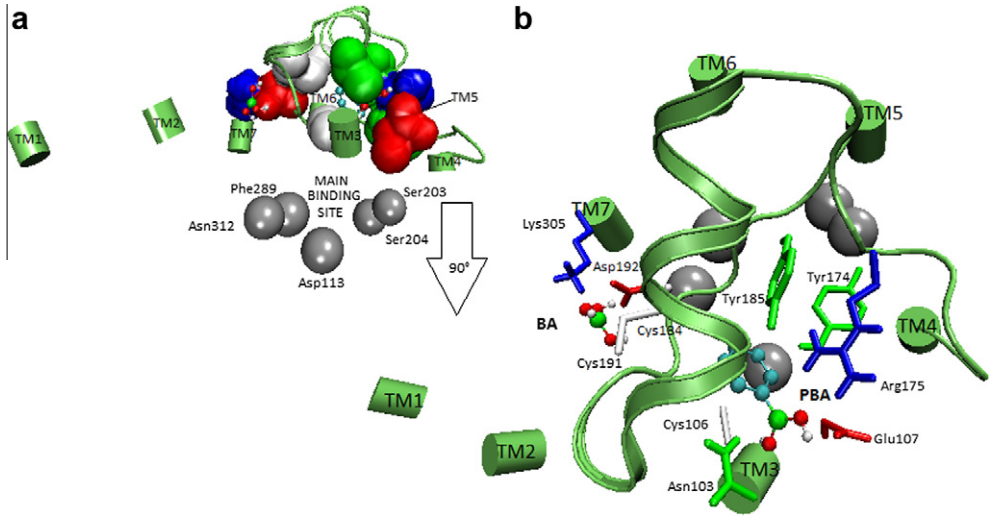

Figure 6. Interaction sites of boric (BA) and phenylboronic (PBA) acids in the highest affinity complexes on hβ_2AR. Residues are colored by type: blue, positive charged; red, negative charged; green, polar uncharged; white, non-polar.

of these facts, the comparative behavior of well-known ligands at the β_2AR allowed us to identify the potencies and efficacies of the compounds tested in this system.

Recent work on drug-β_2AR interactions and the functional consequences indicate the participation of multiple events in these phenomena.[35–37] Our experimental results imply a similar affinity of BCSDs and salbutamol on the hβ_2AR, but maximal hβ_2AR-mediated cAMP accumulation induced by BCSDs was higher than that of salbutamol and similar to that of isoproterenol (Table 1). This partially justifies our previous observations on the smooth-muscle relaxing effect in guinea-pig tracheal rings.[4,5] that the higher potency and efficacy of BCSDs for smooth-muscle relaxation may be related to higher cAMP accumulation.

Changes in the catechol ring by the addition of boron-containing moieties thus did not modify the agonist affinity, but modified the intrinsic activity of hβ_2AR ligands on this cellular system. In this regard, there is increasing evidence that the intrinsic efficacy of hβ_2AR ligands (their capability to induce G protein conformational changes and cAMP formation) involves interactions with and changes in TM5 to TM7 of the receptor, as shown also for other 7TM receptors.[7,37] Unlike their structurally similar precursor salbutamol (a well-known partial agonist), we propose that BCSDs have a great number of interactions with residues in TM5, and that these interactions are critical for the response of these receptors.

Through our experimental approach, we sought to resolve a second issue about BCSDs, that of their stability. Even though we have demonstrated, by an HPLC study, the stability of BR-AEA in rabbit plasma,[38] the stability of boron–ester derivatives in aqueous solution has been questioned.[39,40] If boron–oxygen bonds break by hydrolysis, as shown for similar molecules,[40] free precursors will appear in those compartments where BCSDs were present. We therefore studied the actions of the boron containing precursors on the salbutamol binding site and functional effects. At 100 μM neither precursor had any effect on the salbutamol K_i value, and although a reduction was found both in the maximal effect (−24% and −25% with boric and phenylboronic acid, respectively) and EC_{50} estimates (by 1.89- and 3.15-fold) for salbutamol-induced cAMP accumulation, the intrinsic experimental variation did not allow for statistical significance, although the change in both parameters leads to reduced coupling efficiency or relative efficacy. Hence, the prediction would in this case be that free precursors should decrease the functional effects of BCSDs.

4.2. Theoretical results and experimental-coupling

Experimental data from this work do not agree with the theoretical/experimental values previously inferred by us, in which the affinity of hβ_2AR for BCSDs was five to eight-fold higher than that for salbutamol.[4,5] However, the affinity predictions of the present study, on hβ_2AR 3D structures embedded in lipid membrane, showed a better concordance with the experimental values reported herein. Thus, it can be inferred that the membrane embedding procedure and MD simulations were able to expose subtle but key receptor conformational changes in TM5, TM6 and TM7, which notably improve the docking predictions. For this reason, similar relationships between experimental and calculated affinity values were found in the present study for any ligand with intrinsic activity.

We observed the inward movements of TM5 and TM7 and the outward movement of TM6 in all structures in relation to the main catecholamine-binding site, as described by Cherezov.[10] This observation has already been employed for the development of new hβ_2AR structures with bound agonists.[12,13] Since the movements of these three key domains is directly related to the ability of agonists to bind to the receptor, we can suggest that all receptor structures in this work could be adopting an active conformational state, either quickly or gradually. Therefore, in spite of the high similarity of binding pockets for agonists and antagonists in crystals or models employed for this task,[12,13,36,40] and the limitations of the methodologies of theoretical affinity estimation, the results make clear that an agonist induces an active conformation in these receptors.

In spite of the high similarity between the embedded structures for the hβ_2AR, subtle changes were found in the TM5 in comparison to structures downloaded from the PDB. These changes involve the displacement of side chains of Ser204 and Ser207 residues towards the core of the binding site in the embedded structure in comparison to the corresponding binding site in the crystallographic structure. This is particularly notable in the snapshot obtained at 30 ns MD from the membrane-embedded 3PDS structure, in which BCSDs showed higher affinity than on other conformational states studied (Figs. 4 and 5c).

Differences between ligands with distinct intrinsic activity on βARs have been studied by mutagenesis and theoretical structure-based methods.[7,12,13,41–44] The current status indicates that key features for full intrinsic activity on βARs allow the agonist

to reach the orthosteric site, followed by hydrogen bond interactions with Ser203, Ser204 and Ser207 on the hβ_2AR, or its equivalent serines in the homologous hβ_1AR.[42,43] In support of this idea, a recent work poses the importance for some agonists to reach Ser207 in the G-protein coupling process.[44] Furthermore, it has been reported that in hβ_1AR, the serine equivalent to Ser207 was only reached by full agonists.[42] There are even reports of some boron-containing ligands that reach the binding site and form a covalent bond with Ser203, Ser204 and Ser207.[45–47]

The fact that the antagonist/inverse agonist ICI118,551 reverted the action of BCSDs[4,5] clearly indicates that covalent bonding is not taking place, and that these two types of compounds are competing for the same binding site. However, the BCSD capability to generate complexes with a greater number and type of interactions with TM5 of β_2AR may be involved in the pharmacological behavior of inducing cAMP accumulation. In docking simulations in the present study, BCSDs were capable of establishing an interaction with the three mentioned serines, reaching not only Ser207 in the agonist-bound derived hβ_2AR structures, but also Tyr199 in this same structure after 30 ns of MD. Moreover, the tetravalent boron atom could also be a determinant in interactions with TM5 residues because its partial negative charge could favor the interaction with HO of serines, as proposed for ligands on some enzymes that expose these residues in its catalytic site.[45–47]

In addition to the agonist-induced TM5 inward movement (which could be favored by BCSD moieties exposed towards TM5), the TM6 outward and TM7 inward movements appear to be required for G αs activation and the subsequent adenylyl cyclase catalytic activity stimulation.[7,35,48,49] It is therefore conceivable that these and other changes at the binding site (as the Ile121-Pro211-Phe282 key interaction, the toggle switch Trp286 activation and TM3-TM6 separation) could be a consequence of initial changes in TM3 to TM6 hydrophobic interactions, for which ligand–TM5 interactions are essential.[7,13,14,44,48] All these changes were observed in our models during free-ligand MD and were particularly notable in the forms derived from agonist-bound template 3PDS. Furthermore, observed BCSD interactions support the possibility that these compounds can generate stable active conformational states in this stage. Nevertheless, this event could only be demonstrated by additional long-time MD simulations with comparative analysis of ligand behavior that is coupled to experimental evidence about structural consequences of BCSD binding and direct/indirect effects on G-protein activity.

On the other hand, in theoretical simulations boron-containing precursors of BCSDs docked above the well-defined main binding pocket for catecholamines depicted in Figure 5. In the highest affinity complexes, BA and PBA reached different sites just below the second extracellular loop, but shared the interactions with residues which have partial or formal charges. Their affinity values on these sites were lower than those for well-known ligands, in agreement with our experimental data in that BA or PBA addition had no significant effect on the affinity or intrinsic activity of salbutamol. Despite this, we observed lower levels of cAMP accumulation compared with BCSDs in some of our assays. However, the variability of results was great. As no variants are expected in the hβ_2AR expressed, the variability of results could involve the interaction with a superficial low-affinity site, as depicted in our simulations (Fig. 6). In previous reports it has been proposed that for this region there is an allosteric or second binding site.[32,50] A role of ligand selectivity[7,36,33,51] and of anion binding[52] has also been suggested. Thus, the binding of BA or PBA in this region could disrupt the β_2AR-G protein coupling process or any other cAMP-coupled system present in the studied HEK-293T cells. Further studies addressing the effect of boron containing compounds on these phenomena are required.

5. Conclusions

We have previously demonstrated that BCSDs are capable of relaxing smooth-muscle through a mechanism blocked by the β_2AR antagonist/inverse agonist ICI118,551. Herein, we showed that BCSDs are highly efficacious for inducing cAMP accumulation in cells expressing high levels of hβ_2ARs. This effect could be explained by interactions in TM5 to TM7 of the hβ_2AR, resulting in the greater capability of BCSDs to interact with serines (as do crystallized full agonists on βARs) in TM5 and to enhance the rotation of TM6 and TM7. This brings about the possibility of hβ_2AR-conformational states with a high capability of activating the coupled G protein. Additional experiments and theoretical studies are required to provide further support for this hypothesis.

Boric and phenylboronic acids could act as allosteric modulators of the hβ_2AR-G protein interactions, as suggested by our theoretical simulations. However, this effect is not supported by our experimental data, even at concentrations higher than that possibly yielded by the full hydrolysis of BCSD, which would represent the concentrations required for the maximal functional effects (this work and Refs. 4,5).

Acknowledgments

Partially supported by Cinvestav, Conacyt (Consejo Nacional de Ciencia y Tecnología; Grants 49371M to J.A.A.M., 132353 to J.C.B. and J.T.F., and scholarships to S.U.M.A., M.F.D. and S.C.A.) and Secretaría de Investigación y Posgrado del Instituto Politécnico Nacional. Authors thank the Conacyt-INNOVAPyME Program Support (139391) provided to Instituto Politécnico Nacional and Laboratorio Médico Químico Biológico. Also, JCB received support from ICyTDF and Fundación Miguel Alemán. Finally, we thank the access to computational resources from Centro Nacional de Supercómputo for MD simulations in this study.

Supplementary data

Supplementary data associated with this article can be found, in the online version, at doi:10.1016/j.bmc.2011.11.054.

References and notes

1. Cazzola, M.; Calzetta, L.; Matera, M. G. *Br. J. Pharmacol.* **2011**, *163*, 4.
2. Tashkin, D. P.; Fabbri, L. M. *Respir. Res.* **2010**, *29*, 149.
3. Baker, J. G. *Br. J. Pharmacol.* **2005**, *144*, 317.
4. Soriano-Ursúa, M. A.; Valencia-Hernández, I.; Arellano-Mendoza, M. G.; Correa-Basurto, J.; Trujillo-Ferrara, J. G. *Eur. J. Med. Chem.* **2009**, *44*, 2840.
5. Soriano-Ursúa, M. A.; Correa-Basurto, J.; Amezcua-Gutiérrez, M. A.; Valencia-Hernández, I.; Padilla-Martinez, I. I.; Trujillo-Ferrara, J. G. *Bioorg. Med. Chem. Lett.* **2010**, *20*, 5623.
6. Soriano-Ursúa, M. A.; Trujillo-Ferrara, J. G.; Correa-Basurto, J. *J. Mol. Model.* **2009**, *15*, 1203.
7. Soriano-Ursúa, M. A.; Trujillo-Ferrara, J. G.; Correa-Basurto, J. *J. Med. Chem.* **2010**, *53*, 923.
8. Tafi, A.; Agamennone, M.; Tortorella, C.; Alcaro, S.; Gallina, B.; Botta, M. *Eur. J. Med. Chem.* **2005**, *40*, 1134.
9. Davis, A. P. *Nature* **2010**, *464*, 169.
10. Cherezov, V.; Rosenbaum, D. M.; Hanson, M. A.; Rasmussen, S. G.; Thian, F. S.; Kobilka, T. S.; Choi, H. J.; Kuhn, P.; Weis, W. I.; Kobilka, B. K.; Stevens, R. C. *Science* **2007**, *318*, 1258.
11. Wacker, D.; Fenalti, G.; Brown, M. A.; Katritch, V.; Abagyan, R.; Cherezov, V.; Stevens, R. C. *J. Am. Chem. Soc.* **2010**, *132*, 11443.
12. Rosenbaum, D. M.; Zhang, C.; Lyons, J. A.; Holl, R.; Aragao, D.; Arlow, D. H.; Rasmussen, S. G.; Choi, H. J.; Devree, B. T.; Sunahara, R. K.; Chae, P. S.; Gellman, S. H.; Dror, R. O.; Shaw, D. E.; Weis, W. I.; Caffrey, M.; Gmeiner, P.; Kobilka, B. K. *Nature* **2011**, *469*, 236.
13. Rasmussen, S. G.; Choi, H. J.; Fung, J. J.; Pardon, E.; Casarosa, P.; Chae, P. S.; Devree, B. T.; Rosenbaum, D. M.; Thian, F. S.; Kobilka, T. S.; Schnapp, A.; Konetzki, I.; Sunahara, R. K.; Gellman, S. H.; Pautsch, A.; Steyaert, J.; Weis, W. I.; Kobilka, B. K. *Nature* **2011**, *469*, 175.
14. Rasmussen, S. G.; Devree, B. T.; Zou, Y.; Kruse, A. C.; Chung, K. Y.; Kobilka, T. S.; Thian, F. S.; Chae, P. S.; Pardon, E.; Calinski, D.; Mathiesen, J. M.; Shah, S. T.;

Lyons, J. A.; Caffrey, M.; Gellman, S. H.; Steyaert, J.; Skiniotis, G.; Weis, W. I.; Sunahara, R. K.; Kobilka, B. K. *Nature* **2011**. doi:10.1038/nature10361.
15. Ramos-Jimenez, J.; Soria-Jasso, L. E.; López-Colombo, A.; Reyes-Esparza, J. A.; Camacho, J.; Arias-Montaño, J. A. *Biochem. Pharmacol.* **2007**, *73*, 814.
16. Alexander, S. P. H. *Methods Mol. Biol.* **1995**, *41*, 79.
17. Bhattacharya, S.; Vaidehi, N. *J. Am. Chem. Soc.* **2010**, *132*, 5205.
18. van der Spoel, D.; Lindahl, E.; Hess, B.; Groenhof, G.; Mark, A. E.; Berendsen, H. J. C. *J. Comput. Chem.* **2005**, *26*, 1701.
19. Kandt, C.; Ash, W. L.; Tieleman, D. P. *Methods* **2007**, *41*, 475.
20. Hess, B.; Bekker, H.; Berendsen, H. J. C.; Fraaije, J. G. E. M. *J. Comput. Chem.* **1997**, *18*, 1463.
21. Berendsen, H. J. C.; Postma, J. P. M.; Gunsteren, W. F.; DiNola, A.; Haak, J. R. *J. Chem. Phys.* **1984**, *81*, 3684.
22. Berger, O.; Edholm, O.; Jahnig, F. *Biophys. J.* **1997**, *72*, 2002.
23. Essmann, U.; Perera, L.; Berkowitz, M. L.; Darden, T.; Lee, H.; Pedersen, L. G. *J. Chem. Phys.* **1995**, *103*, 8577.
24. Patra, M.; Karttunen, M.; Hyvonen, M. T.; Falck, E.; Lindqvist, P.; Vattulainen, I. *Biophys. J.* **2003**, *84*, 3636.
25. Van Aalten, D. M.; Bywater, R.; Findlay, J. B.; Hendlich, M.; Hooft, R. W.; Vriend, G. *J. Comput. Aided Mol. Des.* **1996**, *10*, 255.
26. Frisch, M. J.; Trucks, G. W.; Schlegel, H. B.; Scuseria, G. E.; Robb, M. A.; Cheeseman, J. R., et al *Gaussian 03, Revision B. 03*; Gaussian, Inc.: Pittsburgh, PA, 2003.
27. Laurie, A. T.; Jackson, R. M. *Bioinformatics* **2005**, *21*, 1908.
28. Sanner, M. F. *J. Mol. Graphics Modell.* **1999**, *17*, 57.
29. Morris, G. M.; Huey, R.; Lindstrom, W.; Sanner, M. F.; Belew, R. K.; Goodsell, D. S.; Olson, J. A. *J. Comp. Chem.* **2009**, *30*, 2785.
30. Goodford, P. J. *J. Med. Chem.* **1985**, *28*, 849.
31. Humphrey, W.; Dalke, A.; Schulten, K. *J. Mol. Graphics Modell.* **1996**, *14*, 33.
32. Soriano-Ursúa, M. A.; Trujillo-Ferrara, J. G.; Correa-Basurto, J.; Kaumann, A. J. *J. Mol. Model.* **2011**, *17*, 2525.
33. Nygaard, R.; Frimurer, T. M.; Holst, B.; Rosenkilde, M. M.; Schwartz, T. W. *Trends Pharmacol. Sci.* **2009**, *30*, 249.
34. Kolb, P.; Rosenbaum, D. M.; Irwin, J. J.; Fung, J. J.; Kobilka, B. K.; Shoichet, B. K. *Proc. Natl. Acad. Sci. U.S.A.* **2009**, *106*, 6843.
35. Congreve, M.; Langmead, C. J.; Mason, J. S.; Marshall, F. H. *J. Med. Chem.* **2011**, *54*, 4283.
36. Weis, W. I.; Kobilka, B. K. *Curr. Opin. Struct. Biol.* **2008**, *18*, 734.
37. Kobilka, B. K. *Trends Pharmacol. Sci.* **2011**, *32*, 213.
38. Soriano-Ursúa, M. A.; Correa-Basurto, J.; Romero-Huerta, J.; Elizalde-Solis, O.; Galicia-Luna, L. A.; Trujillo-Ferrara, J. G. *J. Enzyme Inhib. Med. Chem.* **2010**, *25*, 340.
39. Wu, S.; Waugh, W.; Stella, V. J. *J. Pharm. Sci.* **2000**, *89*, 758.
40. Hall, D. G. *Structure, properties, and preparation of boronic acid derivatives. Overview of their reactions and applications*; Wiley-VCH Verlag GmbH & Co. KGaA: Weinheim, 2005.
41. Soriano-Ursúa, M. A.; Trujillo-Ferrara, J. G.; Alvarez-Cedillo, J.; Correa-Basurto, J. *J. Mol. Model.* **2010**, *16*, 401.
42. Warne, T.; Moukhametzianov, R.; Baker, J. G.; Nehmé, R.; Edwards, P. C.; Leslie, A. G.; Schertler, G. F.; Tate, C. G. *Nature* **2011**, *469*, 241.
43. Sato, T.; Kobayashi, H.; Nagao, T.; Kurose, H. *Br. J. Pharmacol.* **1999**, *128*, 272.
44. Goetz, A.; Lanig, H.; Gmeiner, P.; Clark, T. *J. Mol. Biol.* **2011**. doi:10.1016/j.jmb.2011.10.015.
45. Transue, T. R.; Krahn, J. M.; Gabel, S. A.; DeRose, E. F.; London, R. E. *Biochemistry* **2004**, *43*, 2829.
46. Stoll, V. S.; Eger, B. T.; Hynes, R. C.; Martichonok, V.; Jones, J. B.; Pai, E. F. *Biochemistry* **1998**, *37*, 451.
47. Di Fiore, A.; Monti, S. M.; Innocenti, A.; Winum, J. Y.; De Simone, G.; Supuran, C. T. *Bioorg. Med. Chem. Lett.* **2010**, *20*, 3601.
48. Moukhametzianov, R.; Warne, T.; Edwards, P. C.; Serrano-Vega, M. J.; Leslie, A. G.; Tate, C. G.; Schertler, G. F. *Proc. Natl. Acad. Sci. U.S.A.* **2011**, *108*, 8228.
49. Yao, X. J.; Vélez, G.; Whorton, M. R.; Rasmussen, S. G.; DeVree, B. T.; Deupi, X.; Sunahara, R. K.; Kobilka, B. *Proc. Natl. Acad. Sci. U.S.A.* **2009**, *106*, 9501.
50. Rosenkilde, M. M.; Benned-Jensen, T.; Frimurer, T. M.; Schwartz, T. W. *Trends Pharmacol. Sci.* **2010**, *31*, 567.
51. Bokoch, M. P.; Zou, Y.; Rasmussen, S. G.; Liu, C. W.; Nygaard, R.; Rosenbaum, D. M.; Fung, J. J.; Choi, H. J.; Thian, F. S.; Kobilka, T. S.; Puglisi, J. D.; Weis, W. I.; Pardo, L.; Prosser, R. S.; Mueller, L.; Kobilka, B. K. *Nature* **2010**, *463*, 108.
52. Shimamura, T.; Shiroishi, M.; Weyand, S.; Tsujimoto, H.; Winter, G.; Katritch, V.; Abagyan, R.; Cherezov, V.; Liu, W.; Han, G. W.; Kobayashi, T.; Stevens, R. C.; Iwata, S. *Nature* **2011**, *475*, 65.
53. Williams, B. R.; Barber, R.; Clark, R. B. *Mol. Pharmacol.* **2000**, *58*, 421.
54. Strange, P. G. *Biochem. Soc. Trans.* **2007**, *35*, 733.